An investigation of ship airwake phenomena using time-accurate CFD and piloted helicopter flight simulation

James S Forrest[*]
Department of Engineering
University of Liverpool
Liverpool, UK
james.forrest@liv.ac.uk

Steven J Hodge[†]
Flight Simulation Department
BAE Systems
Preston, UK
steve.hodge@baesystems.com

Ieuan Owen[‡]
Department of Engineering
University of Liverpool
Liverpool, UK
i.owen@liv.ac.uk

Gareth D Padfield[◊]
Department of Engineering
University of Liverpool
Liverpool, UK
gareth.padfield@liv.ac.uk

This paper describes the use of Computational Fluid Dynamics (CFD) data to improve the fidelity of helicopter-ship dynamic interface simulation. Time-accurate airwakes for the simple frigate shape (SFS2) and a Type 23 Frigate have been computed for a number of wind-over-deck (WOD) angles to provide a realistic flow field in which to perform simulated deck landings within the FLIGHTLAB flight simulation environment. CFD predictions show good agreement with both wind tunnel data and full scale at-sea experimental data. Results from piloted flight trials using the University of Liverpool full-motion simulator are presented in detail. Pilot workload ratings resulting from the trials have been used to generate two Ship-Helicopter Operating Limits (SHOL) diagrams for a Lynx-like helicopter: one operating from the SFS2 and the other from a Type 23 Frigate. Pilot control activity for several WOD cases has been analysed in order to identify the nature of the interactions between airwake turbulence and the helicopter aerodynamic model. It is shown that the location and magnitude of velocity fluctuations on the rotor disk have a significant impact on the control activity required to maintain station over the landing spot. This study builds on earlier work performed at Liverpool and provides a platform for such simulations being used to reduce at-sea trials, and to provide a safe environment for pilot training

Introduction

Landing a helicopter on a ship at sea is one of the most demanding and hazardous tasks that a helicopter pilot can face. Ship-based helicopters routinely operate from a rolling, pitching and heaving flight deck with degraded visibility in close proximity to the ship's superstructure. Additionally, air moving over the ship, due to the combined effects of the ship's forward speed and the prevailing wind, creates a complicated flow field in the lee of the superstructure. This 'airwake' is characterised by turbulent eddies at various scales, by vortices and moving shear layers that combine to buffet the helicopter during approach and landing. The oncoming wind direction and strength has a significant impact on the nature of the airwake. In some conditions the airwake disturbance may lead to pilot workload which is so high, or control margins that are so reduced, that it is unsafe to attempt a landing or take-off.

Safe operating envelopes for helicopter/ship operations, known as the Ship Helicopter Operating Limits (SHOL) are derived through First-of-Class Flight Trials (FOCFTs). These trials require an experienced test pilot to perform a number of deck landings in a variety of wind-over-deck (WOD) conditions giving a subjective workload rating for each test point. Not only is this an inherently dangerous activity, but it is also highly dependent on the prevailing weather conditions. Despite a great deal of prior planning it is often not possible to test every required wind condition, leading to a conservative estimate of the SHOL. At-sea trials are also expensive, requiring the dedicated use of an aircraft and naval assets for weeks at a time.

Research is currently underway to investigate the possibility of reducing the need for at-sea trials when deriving a SHOL. It has been proposed by a number of researchers that high-fidelity piloted simulation might be one possible alternative [1]. The focus of the present study is the use of state-of-the-art CFD techniques to provide ship airwake data for this purpose.

Previous work at the University of Liverpool [2] has shown that the integration of a steady-state CFD airwake model with a FLIGHTLAB helicopter model

[*]Postgraduate Research Student, [†]Senior Engineer, [‡]Professor of Engineering, [◊]James Bibby Professor of Aerospace Engineering. Presented at the 34th European Rotorcraft Forum, Liverpool, UK, September 16 – 19, 2008.

increased pilot workload during the deck landing task in the simulator. Furthermore, the introduction of an unsteady airwake [3] provided an even greater increase in pilot workload and simulation fidelity. These studies used generic ship geometry, the Simple Frigate Shape (SFS/SFS2), to generate the CFD airwake model. More recently this work has been extended through the use of a more realistic ship geometry, a Royal Navy Type 23 Frigate [4].

As well as making improvements to CFD airwake fidelity by performing simulations on a more complex geometry, progress has also been made through the use of a turbulence modelling technique known as Detached-Eddy Simulation (DES) [5]. Much of the work already published on the use of CFD for ship airwakes has used inviscid methods or Reynolds Averaged Navier-Stokes (RANS) methods with some form of turbulence modelling [6]. It has been shown by a number of researchers that RANS methods with standard turbulence models give poor results when applied to bluff-body flow with massive separation [7]. In highly separated regions turbulent eddies are geometry dependent, anisotropic and tend to exhibit unsteady behaviour, so the turbulence models are operating well outside the parameters of their calibration test cases. For these types of flow it would be desirable to resolve the large scales of turbulence using a method such as Large-Eddy Simulation (LES). However, near wall resolution is an issue with this approach and it has been shown that applying LES to high Reynolds number external flows may not be feasible for many years [5].

DES overcomes the limitations of more traditional turbulence models by allowing medium to large turbulent structures to be explicitly resolved by the grid, as opposed to being fully modelled. This allows airwake unsteadiness to be maintained and a more realistic turbulent spectrum can therefore be captured. It has recently been shown [4] that the frequency spectrum of DES generated ship airwakes is closer to experimental data than unsteady RANS methods. DES has also been applied to a wide range of other high Reynolds number external aerodynamic flows and has shown to be equal to, or in many cases better than, RANS for aerodynamic predictions [8].

An unfortunate consequence of moving to more sophisticated methods such as DES is the need to solve on finer computational grids. As grid resolution becomes finer, so the number of computational cells increases and therefore the amount of time required to generate the airwake also increases. This problem is further compounded when the geometry in question is complex, as a more complicated body requires more points to accurately describe it. The amount of time required to 'clean up' and mesh CAD data for a detailed ship model such as the Type 23 Frigate is at least an order of magnitude higher than that of a more generic ship geometry such as the SFS2 (Fig. 1).

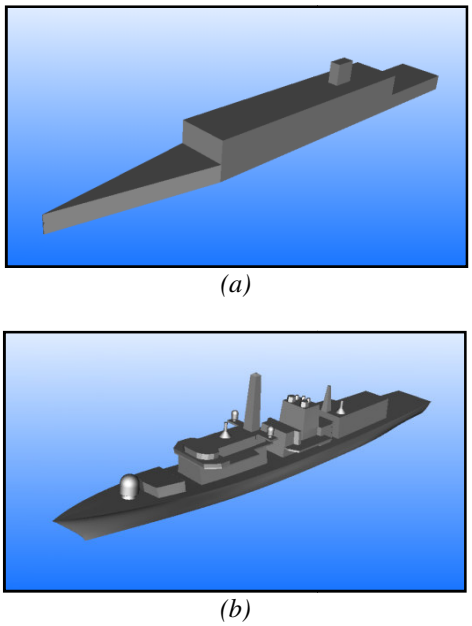

(a)

(b)

Figure 1: Geometries used for computations. SFS2 (a), Type 23 Frigate (b).

A high fidelity airwake model which represents coherent turbulent structures moving in time and space has been integrated into the piloted flight simulation environment. It is important to understand how the interaction of this turbulence with the flight dynamics model affects pilot workload. By gaining an insight into the airwake structures which contribute to aircraft disturbances over the flight deck it may be possible to influence future ship design in order to alleviate workload. The current study is therefore motivated by the desire to develop an understanding of how such airwake flow structures differ at varying WOD conditions, and the resultant effect that this has on pilot workload. A combination of CFD flow field inspection, analysis of pilot ratings and control inputs will be used to link the effects of airwake turbulence with workload.

Computational Approach

The commercial CFD code, FLUENT®, was used for the current study. Second order discretisation was used in time and space, with a blended upwind/central-differencing scheme used for the convective terms. Pressure-velocity coupling was achieved through the use of the PISO scheme.

Due to the complex nature of the problem and the need for time-accurate solutions, the computations were performed in parallel on a high performance computing

cluster consisting of 140 processors. Each computation typically used 32 processors, taking approximately 150 wall clock hours to obtain 45 seconds of airwake data.

A uniform velocity magnitude was specified at the inflow boundary, giving a freestream velocity of 40kts (U_∞ = 20.6m/s). Although the DES turbulence model (discussed below) would be used to capture the majority of the airwake turbulence, a background turbulence field was set by specifying an inlet eddy-viscosity equivalent to 10% turbulence intensity.

In the discussion to follow naval terminology will be used, such that winds from the port side are named 'Red' and those from the starboard side are 'Green'. For example, a 'Green 30' wind describes an incident wind coming from 30° to the right of the ship's bow.

Airwakes consisting of 45 seconds of time-accurate data were generated for both geometries in 15° increments from Red 90, through the headwind, to Green 90. The first 15 seconds of each solution was discarded to allow for initialisation and decay of transients. Airwake data consisting of longitudinal, lateral and vertical velocity components was then written out every 4 time-steps for the next 30 seconds, corresponding to a sampling rate of 20Hz.

Detached-Eddy Simulation

The approach to turbulence modelling used for the current study was proposed by Spalart *et al*. [5] as a response to the failings of standard turbulence models and the unfeasibility of using LES for solving high Reynolds number external flows. It is a modification to the Spalart-Allmaras (S-A) turbulence model such that the distance to the wall, d, is replaced with:

$$\tilde{d} = \min(d, C_{DES}\Delta) \qquad (...1)$$

In the unmodified S-A model d is the length scale which drives the production of eddy-viscosity. By applying the new length scale, $\tilde{d}$, and linking its size to the local grid spacing, Δ, in regions away from walls, eddy viscosity production is limited allowing DES to explicitly resolve medium to large scales of turbulence. The constant C_{DES} has a default value of C_{DES} = 0.65, calibrated in homogeneous decaying turbulence; this value has been retained during the current study.

Mesh generation

The geometries were placed in domains with dimensions chosen such that blockage effects were negligible. The guidelines given in Spalart [9] were followed, and the domains were meshed using an unstructured scheme. It has been shown that unstructured meshes are particularly suitable for DES due to the near isotropic nature of tetrahedra away from solid boundaries [10].

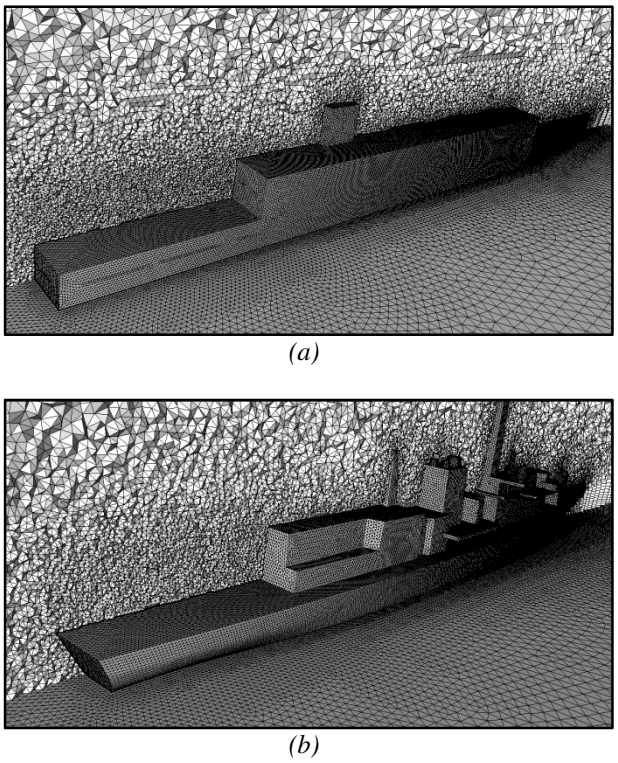

(a)

(b)

Figure 2: Baseline computational meshes. SFS2 (a), Type 23 Frigate (b).

The baseline meshes for the SFS2 and Type 23 (Fig. 2) contained approximately 5.8 million and 6.7 million cells, respectively. The SFS2 geometry was scaled to match the dimensions of the Type 23 by h, hangar height. Surface spacing on and around both flight decks, Δ_0, was set to 0.3m or 0.05h. Size functions were employed to ensure smooth cell growth away from the ship surfaces; cell growth was restricted in the region around the flight deck to provide a 'focus region' of uniformly distributed cells of size Δ_0 to enable the resolution of turbulent structures. Fifteen layers of prisms were attached to the ship surfaces with an expansion ratio of 1.3 to resolve the boundary layer.

In order to study the effects of grid dependency, two further SFS2 meshes were generated by refining and coarsening the baseline grid by a factor of $\sqrt{2}$. This led to a coarse mesh and a fine mesh containing approximately 3.3 million and 10.4 million cells, respectively. A grid dependence study was performed, comparing mean velocity components and turbulent quantities with experimental data. This confirmed that the baseline grid was appropriate.

Time-step

A time-step was chosen to ensure that the local Courant-Friedrichs-Levy (CFL) number did not exceed a value of 1 in the domain. Using $\Delta t = \Delta_0/U_{max}$, and assuming a value of $U_{max} = 1.5U_\infty$ led to Δt = 0.0125s, or 0.019 when non-dimensionalised by beam length and freestream velocity. This is similar to that used by Forsythe *et al*. [11] in their study of flow over the F-15E at stall which also modelled massively separated high Reynolds number flow.

A study to test the sensitivity of the simulation to time-step showed that the value adopted was appropriate. A smaller time-step was shown to resolve more turbulent energy at higher frequencies. However, as these frequencies were outside the typical range of pilot closed-loop response (0.1 – 1Hz), it was felt that the associated increase in required computational time was not justified.

Method validation

A validation study was performed to gain confidence in the accuracy of the CFD modelling by comparing the results obtained using both geometries with experimental data. Data for the SFS2 was obtained from the National Research Council of Canada (NRC) consisting of the results of a comprehensive wind tunnel study. The UK Defense Science and Technology Laboratory (dstl) provided anemometer data derived from at-sea tests for the Type 23 Frigate.

Figures 3 & 4 show contour plots of mean velocity components and turbulence intensities for the SFS2. The CFD colour maps have been scaled to match the experimental maps and both sets of data have been normalised by freestream velocity magnitude. Gaps in the experimental plots indicate regions where reliable hot-wire anemometer measurements could not be taken. The headwind case in Fig. 3 shows excellent agreement, with a clear area of retarded flow behind the hangar face and associated levels of elevated turbulence.

Figure 4 shows a wind from Green 45; a much more challenging test case due to the complexity of the flow field and the presence of separating shear layers. Overall flow topologies are similar, with a large separated wake region to the port side of the flight deck and a concentrated area of turbulence over the port deck edge. The main discrepancy for this case is the prediction of a small separated region over the deck centerline, which is not observed experimentally. The difficulty in predicting separation angles using CFD is well known and may be a factor. An over-prediction of lateral turbulence is also apparent from Fig. 4 (b), which may indicate insufficient damping of the flapping shear layer shed from the windward edge of the hangar face.

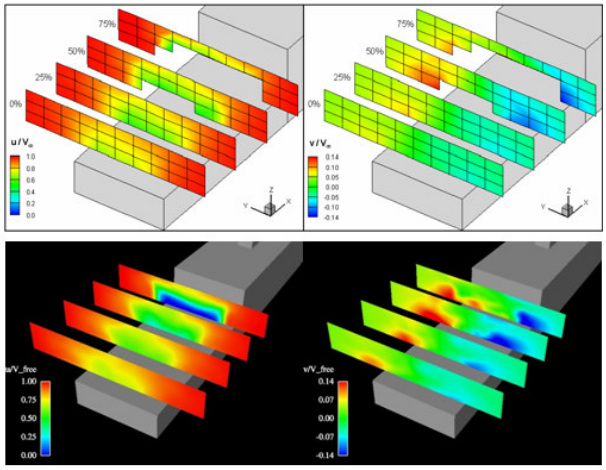

(a)

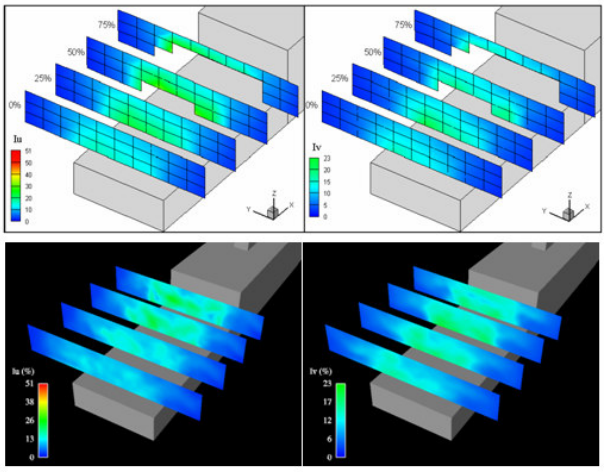

(b)

Figure 3: Comparison of experimental data (top) with CFD results (bottom) for a headwind. Diagram (a) shows longitudinal and lateral velocity components, (b) shows longitudinal and lateral turbulence intensities.

A comparison of the Type 23 results with at-sea data also shows reasonable agreement. Figure 5 shows time-averaged turbulence intensity and velocity data at the various anemometer sample points for a Green 10° wind. Both sets of data are normalised by velocity magnitude at the ship's anemometer. The points are arranged such that they increase in groups of four laterally across the deck from port to starboard. Points 1-4 are closest to the hangar face and 9-12 are furthest aft. Points 10 & 11 are located above the landing spot and all points are situated at hangar height, h = 6m above the deck.

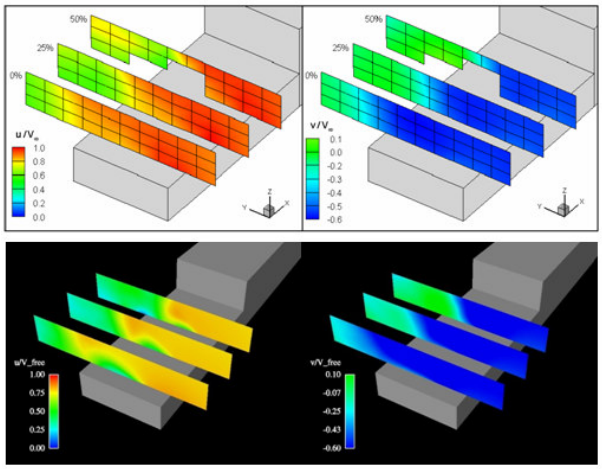

(a)

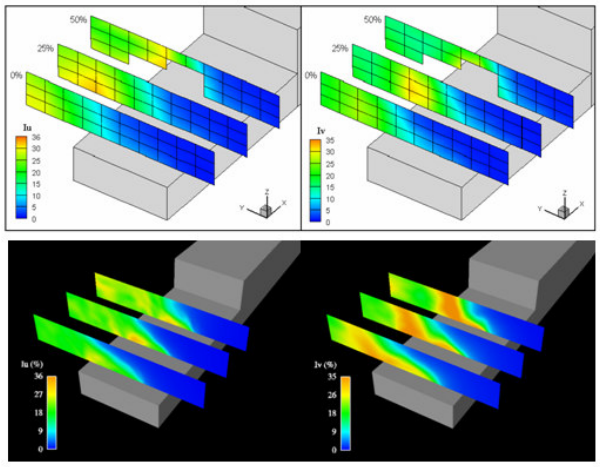

(b)

Figure 4: Comparison of experimental data (top) with CFD results (bottom) for a Green 45° wind. Diagram (a) shows longitudinal and lateral velocity components, (b) shows longitudinal and lateral turbulence intensities.

Unlike the wind tunnel data provided for the SFS2 validation study, the Type 23 experimental data was obtained at sea and is therefore influenced by the Earth's atmospheric boundary layer (ABL). The ABL causes a velocity reduction near the sea surface and a corresponding increase in background turbulence. It was therefore necessary to perform several additional computations which matched these conditions. The following power law model was used to generate an inlet velocity profile:

$$U = U_{ref}\left(\frac{z}{z_{ref}}\right)^{\alpha} \qquad (...2)$$

The constant α was set equal to 0.13 as recommended by Counihan [12] for an ocean surface. The reference height was specified as z_{ref} = 300m above sea level, where the velocity magnitude was set to U_{ref} = 35m/s. A background turbulence intensity of 10% was specified up to a height of 100m, after which it reduced linearly to 1% at 500m.

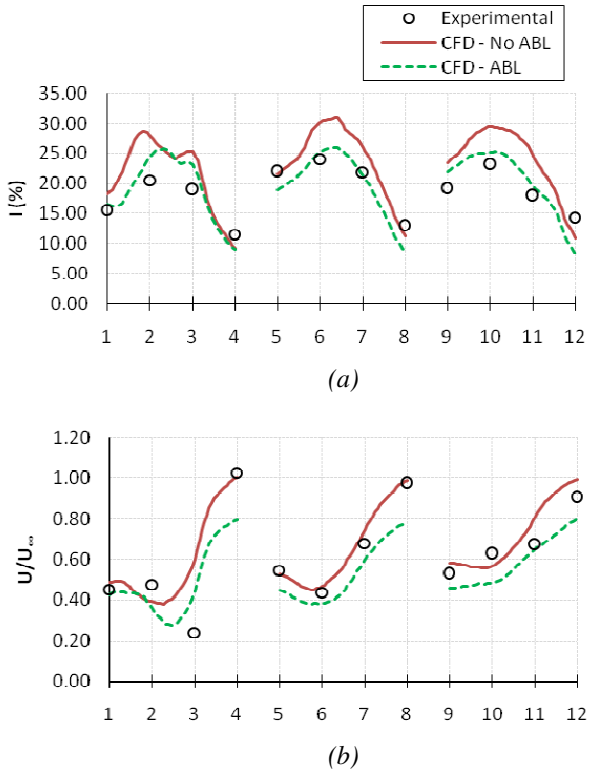

Figure 5: Comparison of Type 23 CFD results with experimental data at anemometer sample points for a Green 10° wind. Turbulence intensity (a), normalised velocity magnitude (b).

It can be seen that while both CFD approaches match the trends well, a significant improvement in the prediction of turbulence levels can be gained from including the effects of the ABL. However, this improvement is not seen in a comparison of velocity magnitudes, with the ABL case under-predicting velocity in the airwake compared to the case computed without the ABL.

These two observations are almost certainly caused by the lower flow speed over the superstructure given by the power law profile. This profile is only an approximation to the at-sea conditions, which would be affected by parameters such as wave height, sea swell and fetch. It is likely that an ABL model which more closely represents the conditions in which the experimental data was obtained would improve results further.

Rotorcraft model

The rotorcraft simulation used for this research is a generic helicopter model configured to be representative of a Westland Lynx helicopter. The simulation model was developed using FLIGHTLAB, an advanced multi-body dynamics modelling and simulation environment, which allows complete rotorcraft simulations to be constructed from a set of modular components e.g. main/tail rotors, fuselage/empennage aerodynamics, landing gear, engines and flight control system blocks. The blade element main rotor model uses five segments for each of the four main rotor blades.

In order for the ship airwake model to affect the flying qualities of the simulated helicopter, the airwake velocity components must be converted into forces and moments at the helicopter's centre-of-gravity. To do this, the airwake velocity components are calculated at a total of 24 Aerodynamic Computation Points (ACPs) distributed around the helicopter. This includes the fuselage and empennage aerodynamic centres, the tail rotor hub and each of the main rotor blade segments.

Airwake integration

The output from the CFD simulations described earlier contains large quantities of time varying data, consisting of the airwake velocity components sampled at each grid point on the unstructured mesh. This data format is unsuitable for direct implementation into a real-time simulation. Therefore, the data at each time-step was interpolated onto a structured grid covering a region around the flight deck and stored in a look-up table format that is compatible with the FLIGHTLAB environment. A series of checks were performed within FLIGHTLAB to confirm that the data processing had not introduced any errors.

Piloted Simulation Results

The results presented in this section were obtained from a series of piloted simulation experiments conducted on the University of Liverpool's HELIFLIGHT facility. The HELIFLIGHT system is a 6 degree of freedom, motion base flight simulator configured with helicopter flight controls. Motion feedback to the pilot is via movement of the platform and through a high-resolution visual system. A more detailed description of the HELIFLIGHT simulator can be found in Padfield & White [13].

The flight test programme consisted of a series of deck landing tasks using airwakes from both ship geometries for winds from Red 90° to Green 90°, through the headwind, in 15° increments. The computed airwake data for each wind angle was scaled both in magnitude and time to allow WOD speeds from 30kts to 60kts to be tested. Polsky [14] has shown that it is valid to scale airwake velocity components within a limited Reynolds number range due to self-similarity. Scaling in time is based on the recognition that bluff-body flows exhibit behavior such that higher incident velocities give rise to higher frequency wake turbulence. A Strouhal type relationship was assumed in this instance.

During each experiment a highly experienced former Royal Navy test pilot was instructed to fly the deck landing task using, as far as possible, standard Royal Navy technique. This involves flying the helicopter to a stabilised hover on the port side of the ship, then manoeuvring sideways across the deck to a position above the landing spot and waiting there for a quiescent period in the ship's motion before executing a vertical landing.

Three key Mission Task Elements (MTEs) were identified from the deck landing mission (Fig. 6):

1) *Approach/sidestep manoeuvre.*
2) *Station-keeping over the deck.*
3) *Vertical landing.*

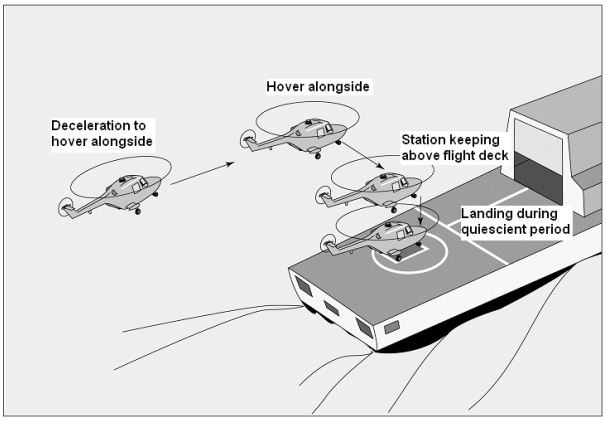

Figure 6: Final stages of the recovery of a Royal Navy helicopter to a single spot frigate.

The pilot quantified the workload during each deck landing, for each of the MTEs described above, using the Deck Interface Pilot Effort Scale (DIPES) (Fig. 7) and the 10-point Bedford workload rating scale [15]. On the Bedford scale, a rating in the range 1-3 is assigned to tasks that present little difficulty. More difficult tasks that reduced the pilot's spare capacity to perform ancillary tasks are awarded increasingly higher ratings. At conditions for which the pilot is not able to apply sufficient effort and has to abandon the task, a rating of 10 is awarded.

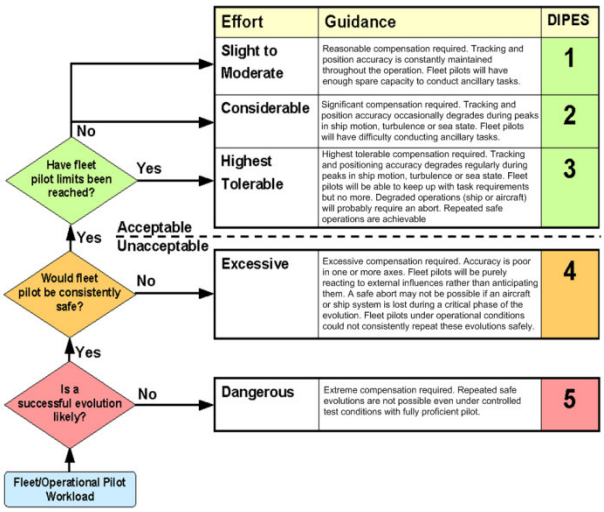

Figure 7: The Deck Interface Pilot Effort Scale (DIPES).

SHOL definition

A SHOL chart defines a set of WOD conditions under which a deck landing may be attempted for a given ship-helicopter combination. SHOLs must be defined for conditions such as day/night, various aircraft weights and sea-states. The typical Royal Navy approach is to use the 5-point DIPES scale to define this envelope. Under DIPES ratings the pilot must take into account both workload and aircraft control margins. There may be cases where workload is low, but control margins are eroded in one or more axis (or vice-versa), in which case a limit will be found. DIPES ratings of 1-3 are deemed acceptable, while 4-5 are outside the SHOL. This enables a boundary to be defined.

Based on the given DIPES ratings from the simulated landing tasks, and taking into account a lateral velocity envelope of 30kts for the Lynx, a fully simulated SHOL has been defined for a Lynx-like aircraft operating to the SFS2 and a Type 23 Frigate (Fig. 8). It is interesting to note that the SHOL boundaries were found to be identical for the SFS2 and the Type 23. This is partly to be expected due to the similarity of the two geometries in the landing deck region, but is also a result of the coarseness of the DIPES scale. Recent work by the current authors [16] has shown that, for the same WOD angle, relatively subtle differences in ship geometry can give rise to significantly different flow features. The location and magnitude of turbulent structures over the flight deck differed between the two geometries studied. By plotting pilot ratings on the 10-point Bedford workload rating scale a corresponding difference in workload was seen, despite the fact that the DIPES ratings were identical. This suggests that the DIPES scale is too coarse to detect certain differences in airwake structure.

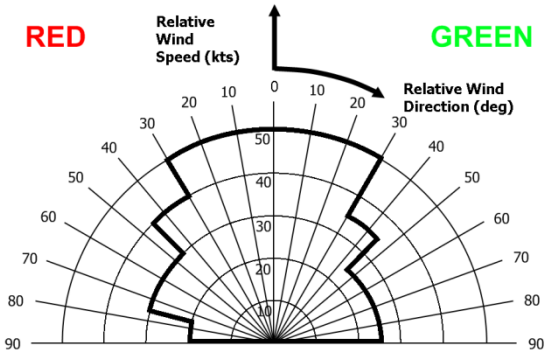

Figure 8: SHOL diagram for a Lynx-like aircraft operating from a Type 23 Frigate or the SFS2.

Pilot workload analysis

A major benefit of performing flight trials within a simulated environment is the ability to record a wealth of flight data. One of the aims of the current work is to gain an insight into the nature of ship airwake turbulence through analysis of pilot response and control strategies employed during the deck landing task. Although pilot comments and workload rating scores are invaluable during comparative studies or qualification purposes, they rarely permit in-depth analysis. This is partly due to their subjective nature, but also due to the limited number of ways in which workload scores can be evaluated. The following section will review flight test data from the deck landing task in an attempt to identify differences in workload between WOD angles. In identifying the nature of disturbances which are responsible for the reported workload it will be possible to validate the pilot responses and also gain a better understanding of ship airwake turbulence.

Figure 9 shows Bedford workload ratings for the Type 23 Frigate as awarded for the station keeping task. The station keeping task has been chosen for presentation as it requires the pilot to maintain station over the deck within the influence of the airwake for a long period of time, regardless of whether the wind is coming from port or starboard. It can be seen that workload increases with WOD speed. This is to be expected as an increase in freestream velocity results in turbulence with greater magnitude and frequency behind the superstructure. Additionally, winds either side of the headwind are shown to increase workload. This can be attributed to the presence of shear layers shed from the hangar roof and edges which are one of the primary mechanisms for airwake turbulence generation.

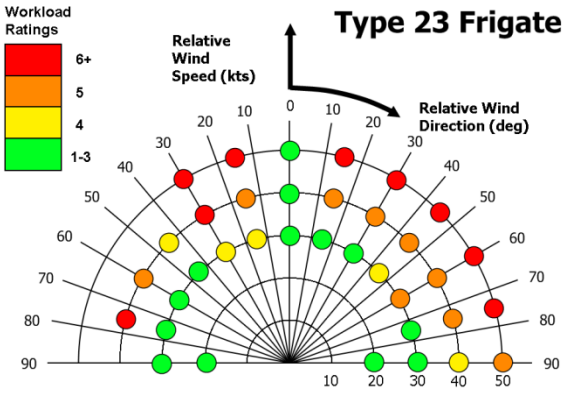

Figure 9: Bedford workload ratings given at each test condition for the station keeping task.

For the purposes of this study it is convenient to choose two WOD conditions which have been given significantly different workload scores by the pilot, as a contrast in workload rating should also indicate a dissimilar airwake structure. Therefore, it was decided that the headwind and Green 45˚ WOD angles would be analysed, both for WOD speeds of 50kts. The test pilot gave the headwind case a rating of 3, classified as "Enough spare capacity for all additional tasks". The Green 45 case was given a rating of 7, classified as "Very little spare capacity, but maintenance of effort on the primary task not in question".

It is instructive to look at a visualisation of the flow fields at the chosen WOD angles in order to determine what may be causing the differences in workload. Figure 10 shows contours of turbulence intensity on a plane at 6m above the flight deck. This is the approximate height of the rotor disk during the translation and station keeping tasks. The approximate location of the rotor disk during the station keeping task is shown as a red circle. A marked difference in flow fields can be seen. For the headwind, turbulence is moderate over the whole of the flight deck, whereas the Green 45˚ case shows a flight deck bisected by a region of high turbulence which is shed from the windward hangar edge. Although at Green 45˚ much of the velocity field experienced by the rotor disk is at freestream conditions, the region between 180˚ and 330˚ azimuth is subjected to levels of airwake turbulence with peak vertical velocity magnitudes up to 75% higher than the headwind case. Due to the 90˚ phase shift this turbulence is likely to cause lift fluctuations at the rear of the rotor disk, leading to significant disturbances in pitch.

Evidence of correction in pitch during the simulation flight trials can be seen in Fig. 11, where traces of cyclic control input are plotted for both cases. Large amplitude inputs are seen in both longitudinal and lateral axes for the Green 45˚ task. In addition, there appears to be a need to keep the stick forward in order to maintain longitudinal position over the spot. Cyclic control inputs are minimal for the headwind case, with only the lateral axis seeing any significant activity.

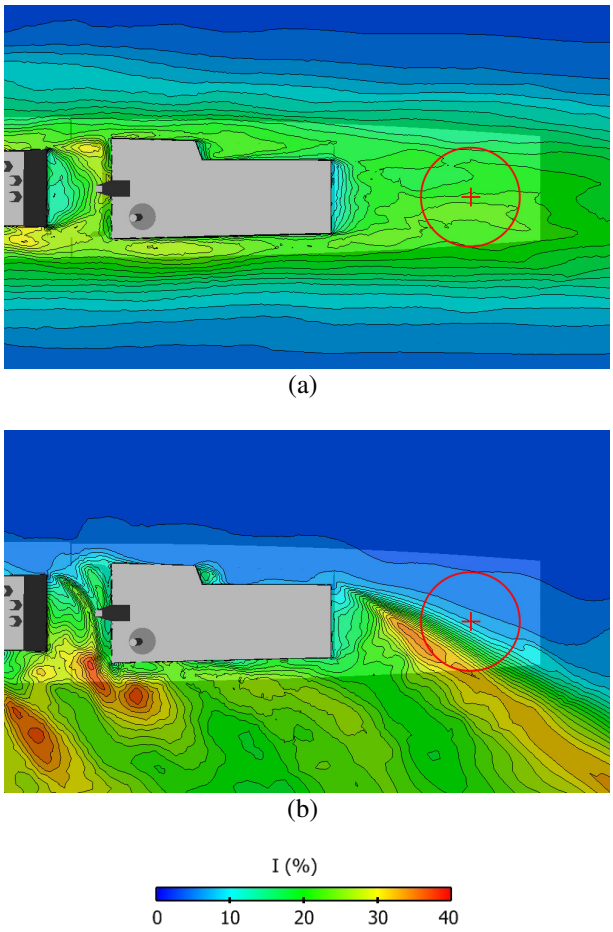

Figure 10: Contours of turbulence intensity plotted at a height of 6m above the flight deck. Approximate location of rotor disk during station keeping task denoted by red circle. Headwind (a); Green 45˚ (b).

The need to maintain forward cyclic during the Green 45˚ case warrants further investigation in order to determine whether this is an airwake related effect. Figure 12 shows contours of mean vertical velocity at the rotor disk during hover. An updraft of up to 4m/s can be seen towards the starboard side of the rotor disk, between 30˚ and 170˚ azimuth. This is caused by flow passing up and over the flight deck at its windward edge. Flow with a positive vertical component entering the starboard side of the rotor disk will increase the effective angle of attack of the blades and, due to the 90˚ phase shift, cause the disk to tilt back. This would require correction in longitudinal cyclic by pushing the

stick forwards in order to prevent the aircraft from moving backwards. This is a relatively constant phenomenon as Fig. 10(b) shows that there is very little turbulence at the port side of the flight deck, hence the requirement to maintain a mean stick position of approximately 20% of forward travel (Fig. 11). This indicates that both mean and unsteady flow features contribute to control strategy during the landing task.

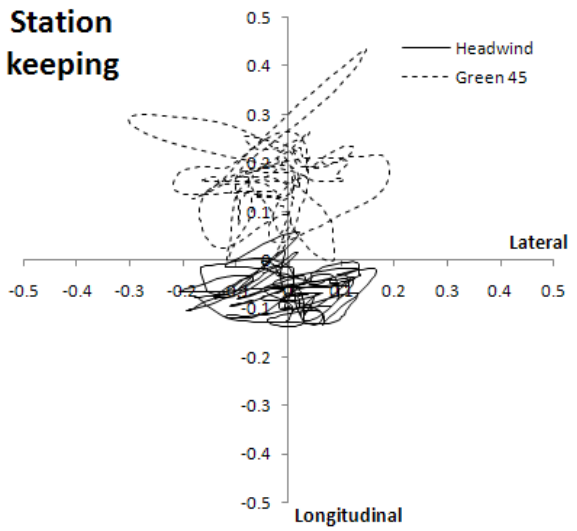

Figure 11: Trace showing cyclic control inputs during the station keeping task. A distance of 0.5 corresponds to 50% of the full travel in each direction.

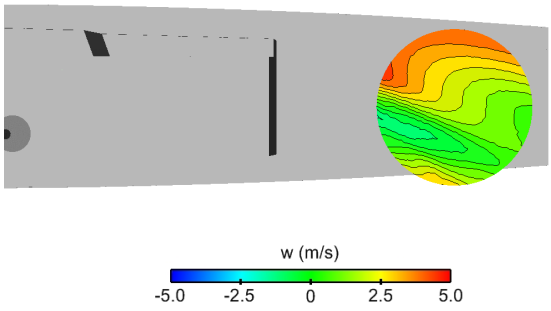

Figure 12: Contours of mean vertical velocity at the estimated location of the rotor disk during hover for the Green 45˚ case.

This difficulty in maintaining longitudinal position during the Green 45˚ case is also seen in Fig. 13. Here the aircraft's location relative to the landing spot in an *x-y* plane is plotted for the station keeping task. It can be seen that during the headwind condition the pilot is able to maintain relatively good control of the aircraft, keeping within a 2m x 2m zone around the landing spot. In contrast, the Green 45˚ case shows a large excursion in the *x* direction corresponding to a total displacement of 5m longitudinally during the 15 seconds of the task. In agreement with the control activity shown in Fig. 11, lateral displacement during the Green 45˚ case is only slightly greater than for the headwind case.

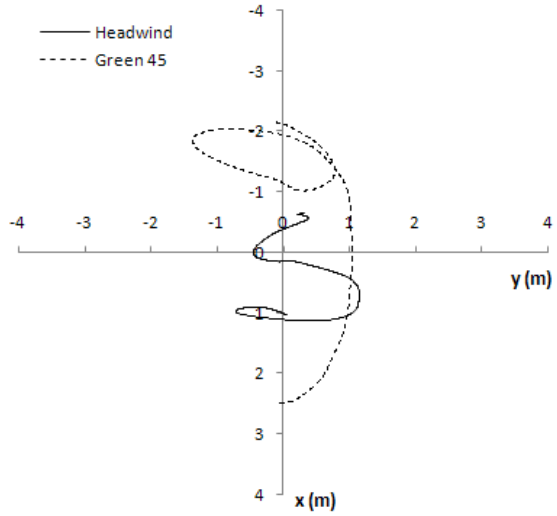

Figure 13: The aircraft's ground track relative to the landing spot during the station keeping task.

To further illustrate the difference in cyclic activity for the two cases studied, Fig. 14 shows Power Spectral Density (PSD) plots for both longitudinal and lateral activity. Both plots show that the majority of activity is within the pilot closed-loop response frequencies of 0.1Hz – 1Hz. However, as seen previously, the level of activity is higher in the longitudinal axis during the Green 45˚ case, particularly to the lower end of the frequency spectrum.

It was stated previously that the increased longitudinal cyclic activity seen for the Green 45˚ case was due to airwake turbulence on the port side of the rotor disk causing fluctuations in pitch. It is well known that the vertical velocity component is dominant in this situation, by changing the induced velocity distribution and hence the effective angle of attack of the blades [17]. Figure 15 shows contours of instantaneous vertical velocity at an estimated rotor disk location during the station keeping task. Figure 15(a) shows that there are moderate spatial velocity variations and pilot comments suggest that some airwake turbulence at the headwind condition is felt, but it is at a magnitude which is manageable, hence the Bedford score of 3. In contrast, Fig. 15(b) shows high vertical velocities, both positive and negative, on the rotor disk between 210˚ and 310˚; the most severe gradient occurs at approximately 270˚ azimuth. It is clear that the location and magnitude of these velocity fluctuations are driving the pitch disturbances seen during the Green 45˚ case.

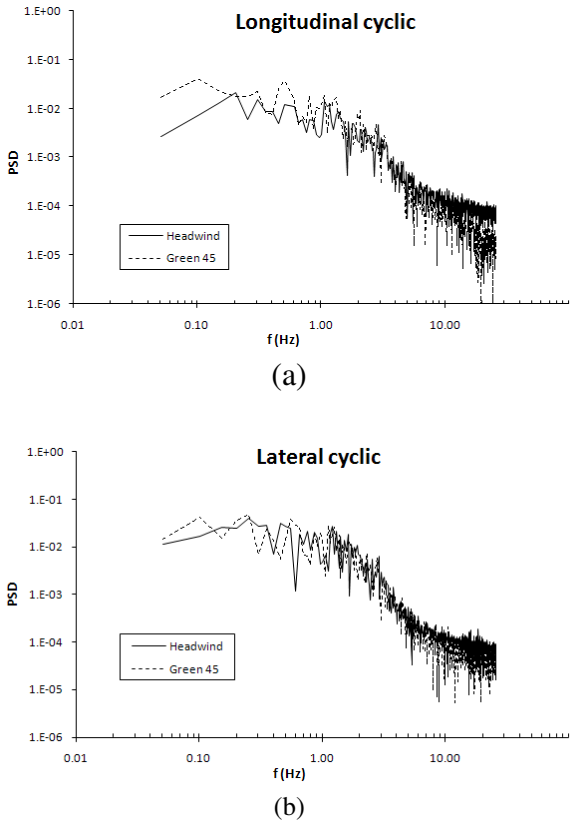

Figure 14: Power Spectral Density plot showing cyclic activity for the headwind and Green 45˚ cases during the station keeping task. Longitudinal (a); lateral (b).

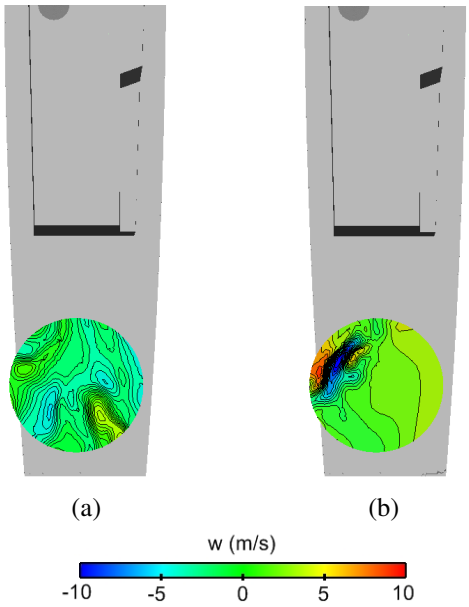

Figure 15: Contours of instantaneous vertical velocity at the estimated location of the rotor disk at hover. Headwind (a); Green 45˚ (b).

Rotor downwash/airwake coupling

The approach to dynamic interface testing presented in this paper can be classed as 'one-way', in that the fully coupled interaction between the ship airwake and rotor downwash is not modelled within the simulations. It has been suggested by some researchers that the use of this approach may be questionable due to the unsteady, non-linear nature of the coupled flow-field [1,18]. However, off-line investigations into two-way coupling have shown that the orientation of airwake vortices is an important factor; those with a horizontal axis of rotation are more likely to be affected by rotor downwash than those oriented vertically [18].

Although it is likely that the structure of airwake turbulence as discussed in this paper would be affected in some way by rotor downwash, it is impossible to predict the resultant effect on pilot workload without a detailed investigation. Real-time, fully coupled piloted simulations are a long term goal of this work, though limitations in available computing power make this currently unfeasible. In the mean time, one-way coupled simulations are a valuable tool in understanding the nature of ship airwake turbulence and its effect on pilot workload and control strategy.

Conclusions

A series of simulation trials have been carried out to assess pilot workload for the deck landing task to a single spot frigate. CFD generated ship airwakes have been computed for this purpose using the highly simplified SFS2 and a reasonably realistic Type 23 Frigate geometry.

Bedford workload rating scores were obtained for three MTEs, which showed that pilot workload varies dramatically depending on the particular WOD condition. By inspecting both statistical and instantaneous aspects of the CFD generated flow fields and comparing this with analysis of pilot control inputs, it has been possible to identify the mechanisms which lead to disturbances at the rotor disk. It has been shown that the location and magnitude of vertical velocity perturbations has a significant impact on both transient control inputs and also the mean stick displacements required to maintain trim.

This type of analysis has been made possible through the use of high fidelity, unsteady ship airwakes which capture medium to large scale coherent flow structures. The use of such airwake data in piloted flight simulation is a key step towards gaining a better understanding of the complex interactions at the ship-helicopter dynamic interface.

Acknowledgements

The first author is jointly funded by an EPSRC Doctoral Training Award and Westland Helicopters Ltd. ANSYS Inc have been most generous in their assistance with licenses. The authors would also like to thank the test pilot, Andy Berryman, for his professionalism and guidance; and Mark White, Steven Kendrick and Neil Cameron from the Flight Science and Technology research group for their help with the simulator. The FLIGHTLAB helicopter model was based on a version of the Lynx provided by QinetiQ. The SFS2 validation data was derived by the National Research Council Canada, and provided under the The Technical Cooperation Program (TTCP) by dstl. The Type 23 Frigate validation data was also provided by dstl.

References

[1]Zan, S.J., On aerodynamic modelling and simulation of the dynamic interface, *Proceedings of the Institution of Mechanical Engineers, Part G: Aerospace Engineering*, 2005, **219**, pp 393-410.

[2]Roper, D.M., Hodge, S.J., Owen, I., and Padfield, G.D., Integrating CFD and piloted simulation to quantify ship-helicopter operating limits, *The Aeronautical Journal*, 2006, **110**, (1109), pp 419-428.

[3]Hodge, S.J., Padfield, G.D., and Southworth, M.R., Helicopter-ship dynamic interface simulation: Fidelity at low-cost, *Cutting Costs in Flight Simulation - Balancing Quality and Capability*, RAeS Conference, London, UK, 2006.

[4]Forrest, J.S., Owen, I., Padfield, G.D., and Hodge, S.J., Detached-Eddy Simulation of ship airwakes for piloted helicopter flight simulation, *1st International Aerospace CFD Conference*, Paris, France, June 18-19, 2007.

[5]Spalart, P.R., Jou, W-H., Strelets, M., and Allmaras, S.R., Comments on the feasibility of LES for wings and on a hybrid RANS/LES approach, *1st AFOSR International Conference on DNS/LES*, Ruston, LA, 1997.

[6]Reddy, K.R., Toffoletto, R., and Jones, K.R, Numerical simulation of ship airwake, *Computers & Fluids*, 2000, **29**, pp 451-465.

[7]Spalart, P.R., Strategies for turbulence modelling and simulations, *International Journal of Heat and Fuid Flow*, 2000, **21**, pp 252-263.

[8]Strelets, M., Detached Eddy Simulation of massively separated flows, *39th AIAA Aerospace Sciences Meeting and Exhibit*, Reno, NV, 2001.

[9]Spalart, P.R., Young-person's guide to Detached-Eddy Simulation grids, NASA Report NASA/CR-2001-211032, 2001.

[10]Morton, S.A., Forsythe, J.R., Squires, K.D., and Wurtzler, K.E., Assessment of unstructured grids for Detached-Eddy Simulation of high reynolds number separated flows, *Proceedings of the 8th International Conference for Numerical Grid Generation in Computational Field Simulations*, International Society for Grid Generation, 2002, pp 571-586.

[11]Forsythe, J.R., Squires, K.D., Wurtzler, K.E., and Spalart, P.R., Detached-Eddy Simulation of the F-15E at high alpha, *Journal of Aircraft*, 2004, **41**, (2), pp 193-200.

[12]Counihan, J., Adiabatic atmospheric boundary layers: A review and analysis of data from the period 1880-1972, *Atmospheric Environment*, 1975, **9**, pp 871-905.

[13]Padfield, G.D. and White, M.D., Flight simulation in academia – HELIFLIGHT in its first year of operation at the University of Liverpool, *The Aeronautical Journal*, 2003, **107**, (1075), pp 529-538.

[14]Polsky, S.A. and Bruner, C.W., Time-accurate computational simulations of an LHA ship airwake, AIAA Paper 2000-4126, *18th Applied Aerodynamics Conference and Exhibit*, Denver, CO, 14-17 August, 2000.

[15]Roscoe, A.H. and Ellis, G.A., A subjective Ratings scale for assessing pilot workload in flight: A decade of practical use, RAE Technical Report TR90019, 1990.

[16]Forrest, J.S., Hodge, S.J., Owen, I., and Padfield, G.D., Towards fully simulated ship-helicopter operating limits: The importance of ship airwake fidelity, *American Helicopter Society 64th Annual Forum*, Montréal, Canada, 29 April – 1 May, 2008.

[17]Padfield, G.D. *Helicopter Flight Dynamics*, Blackwell, 2007.

[18]Bridges, D.O., Horn, J.F., Alpman, E., and Long, L.N., Coupled flight dynamics and CFD analysis of pilot workload in ship airwakes, AIAA Paper 2007-6485, *AIAA Atmospheric Flight Mechanics Conference and Exhibit*, Hilton Head, SC, 20-23 August, 2007.